Civil Engineering Infrastructures Journal, 49(2): 347 – 359, December 2016
Print ISSN: 2322-2093; Online ISSN: 2423-6691
DOI: 10.7508/ceij.2016.02.011

Technical Note

Investigation of Utilizing a Secant Stiffness Matrix for 2D Nonlinear Shape Optimization and Sensitivity Analysis

Vatani Oskouie, A.[1*] and Havaran, A.[2]

[1] Associate Professor, Faculty of Civil Engineering, Shahid Rajaee Teacher Training University, Tehran, Iran.
[2] Ph.D. Candidate, Faculty of Civil Engineering, Shahid Rajaee Teacher Training University, Tehran, Iran.

Received: 08 Jan. 2016; Revised: 13 Oct. 2016; Accepted: 18 Oct. 2016

ABSTRACT: In this article the general non-symmetric parametric form of the incremental secant stiffness matrix for nonlinear analysis of solids have been investigated to present a semi analytical sensitivity analysis approach for geometric nonlinear shape optimization. To approach this aim the analytical formulas of secant stiffness matrix are presented. The models were validated and used to perform investigating different parameters affecting the shape optimization. Numerical examples utilized for this investigating sensitivity analysis with detailed discussions presented.

Keywords: Nonlinear Analysis, Optimization, Prescribed Displacement, Sensitivity Analysis.

INTRODUCTION

Structural optimization utilizing Linear static sensitivity analysis has been used since many years ago (Kim et al., 2012; Choi and Kim, 2005; Van Keulen et al., 2005). The Finite Element method is an effective tool for these analyses and has been utilized for years. The extensive use of numerical integration makes the analysis straightforward, but as material, elements and system are often given in different co-ordinate systems, the analysis involves many rotational transformations. The most common methods to gain sensitivities are the global finite difference method, the variational method and the discrete method (Kim et al., 2012; Choi and Kim, 2005; Van Keulen et al., 2005; Pedersen, 2005; Tromme et al., 2015). The implementation of the global finite difference method is straightforward. However, the method has some deficiency when the size is either too large or too small, and, it become worse in the repeated, time-consuming structural analyses. In this study the discrete method is considered due to the convenience of a straightforward utilizing the finite element codes (Pedersen, 2005). Because of the analytical derivatives of discrete quantities such as the stiffness matrix, mass matrix, and load vector, are difficult to achieve, semi-analytical methods, where analytical derivatives are approximated by finite

* Corresponding author E-mail: vatani@srttu.edu

differencing, have been widely employed (Pedersen, 2005). The simple three-node triangular element with uniform strain, stress, thickness, and material moduli is chosen. This element is often utilized in design optimization and imply rather simple final stiffness matrices. Earlier works (Pedersen and Cederkvist, 1981) on analytically obtained stiffness matrices for finite-element modeling are here improved to include geometrical non-linearity based on the Green Lagrange strain definition. Recent work of Rezaiee-Pajand and Yaghoobi (2015) utilized the complete second-order function to formulate the quadrilateral elements. According to Pedersen and Cederkvist (1981); Zienkiewicz and Taylor (2000) and Pedersen (2005) the present nonlinear Finite Element method is independent on stress-strain state and material and a few basic matrices describe the element geometry, orientation, nodal positions, and displacement assumption. Stiffness matrices established from linear combinations of the basic matrices which have extracted from material parameters and displacement gradients parameters (Pedersen, 2005). Investigation of an accurate geometric nonlinear sensitivity analysis method utilizing a secant stiffness matrix have presented in this article.

First, the tangent stiffness matrix and, the secant stiffness matrix utilized in the proposed nonlinear analysis procedure are introduced, then the discrete semi-analytical sensitivity analysis in conjunction with the adjoint approach is described, after that the exact semi-analytical sensitivity analysis method is extended to the nonlinear case, and, the sensitivity results of reaction force and influence of mesh sizes for a cantilever beam problem are discussed, and finally the conclusions are presented.

MATERIALS AND METHODS

Definition of Secant and Tangent Stiffness Matrix in Nonlinear Analysis

Generally, the governing equation of a Finite Element system is:

$$K.U = F \tag{1}$$

where K: is the stiffness matrix, U: is the nodal displacement vector, and F: is the external force vector. In nonlinear method, the stiffness matrix K has nonlinear relationships with U, and Eq. (1) becomes:

$$K_S(U).U = F \tag{2}$$

where K_S: is secant stiffness matrix, which depends on both U and the structure's initial condition. Another important quantity is the tangent stiffness matrix K_T, which is also nonlinearly dependent on U and structure's configuration. In a nonlinear analysis method, the secant stiffness matrix utilizes to compute the residual force vector, while the tangent stiffness matrix is mainly used to determine the incremental quantities. A descriptive figure of K_S and K_T is depicted in Figure 1 (Pedersen, 2005).

Figure 2 presents a triangular element which parameterized by the parameters p_2–p_5. A parameter p_1 is used for axisymmetric elements, in this paper the plane linear displacement triangle utilized for plane problems in co-ordinate system with axis x,y. Translation of the element has no influence on the element stiffness parameters and also the element size, characterized by a length parameter h, is without influence (Pedersen, 2005). The area (a) of the element is determined by:

$$a = 1/2\,(p_2p_5 - p_3p_4 > 0 \tag{3}$$

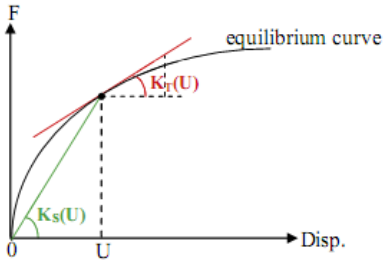

Fig. 1. Definition of Secant K_S and tangent K_T stiffness (Pedersen, 2005)

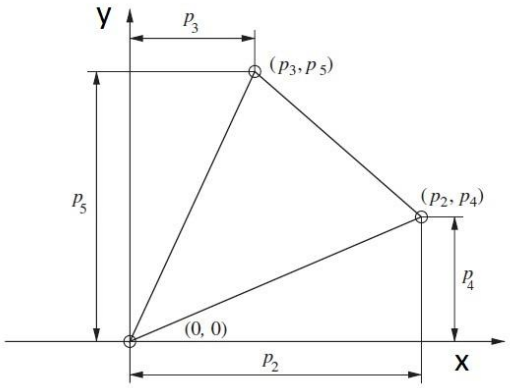

Fig. 2. Definition of parameters p_2–p_5, that describe the triangle shape. The order of the three nodes are restricted by $p_2p_5 - p_3p_4 > 0$ (Pedersen, 2005)

The constant thickness of the element is t. Although the co-ordinates of the Cartesian co-ordinate system is chosen as *x,y* the *i*, *j* index notation is also used meaning that *i* can be x or y and similar for *j* in this two-dimensional description. Displacement of v_i in the *i* direction is obtained as:

$$v_i = \{H\}^T[K]^{-1}\{D\}_i = \{N\}^T\{D\}_i \quad (4)$$

where the vector $\{D\}_i$: is the nodal displacements in direction *i*. Thus, only no-directional coupling is used in the interpolation for problems. However, the same displacement assumption is utilized in all directions, interpolation $\{N\}$ without index *i*. The vector $\{N\}$ of shape functions factorized into the vector of direct displacement assumptions $\{H\}$ and the space-independent matrix $[K]^{-1}$ which includes information about element geometry and node positions. Dealing with a linear displacement assumption in the *x,y* co-ordinate system Eq. (5) is obtained as follows:

$$\{H\}^T = \left\{1 \ \frac{x}{h} \ \frac{y}{h}\right\} \quad (5)$$

where *h*: is a reference length, which has no impact in the final results. The displacement gradients $v_{x,x}$, $v_{x,y}$, $v_{y,x}$ and $v_{y,y}$ are, with $[K]^{-1}$ space-independent, given by:

$$v_{x.x} = \{H\}^T{}_x[K]^{-1}\{D\}_{x.} \quad (6)$$
$$v_{x.y} = \{H\}^T{}_y[K]^{-1}\{D\}_{x.} \quad (7)$$
$$v_{y.x} = \{H\}^T{}_x[K]^{-1}\{D\}_{y.} \quad (8)$$
$$v_{y.y} = \{H\}^T{}_y[K]^{-1}\{D\}_{y.} \quad (9)$$

where for instance $\{H\}_{,x}$ means differentiation of all the components in $\{H\}$ with respect to the coordinate x. From Eq. (5) follows the involved vectors:

$$\{H\}^T_{.x} = \left\{0 \ \frac{1}{h} \ 0\right\} \ and \ \ \{H\}^T_{.y} = \left\{0 \ 0 \ \frac{1}{h}\right\} \quad (10)$$

The matrix $[K]$ constitutes the row vectors $\{H\}^T$ considered at the three nodal positions, and thus is independent of space. The inverse of this matrix is (Pedersen, 2005):

$$[K]^{-1} = \frac{1}{2a}\begin{bmatrix} p_2p_5 - p_3p_4 & 0 & 0 \\ (p_4 - p_5)h & p_5h & -p_4h \\ (p_3 - p_2)h & -p_3h & p_2h \end{bmatrix} \quad (11)$$

Definition of Linear Strains and Basic Matrices

The present formulation follows mentioned by Pedersen and Cederkvist (1989) with extensions as presented in Cheng and Olhoff (1993) for 2D problems applied to linear elastic behavior and small strains. As later shown in detail with Green–

Lagrange strains the final directional stiffness submatrices can be evaluated as linear combinations of the material moduli and basic matrices $[T_{ij}]$ is defined by:

$$[T_{ij}] := [K]^{-T} \int \{H\}_{.i} \{H\}^{T}{}_{.j} \, dV \, [K]^{-1} \quad (12)$$

which with the already given matrices $\{H\}$, j and $[K]^{-1}$, that are constant in the element, is determined to:

$$[T_{xx}] = \frac{t}{4a} \begin{bmatrix} (p_4 - p_5)^2 & p_5(p_4 - p_5) & -p_4(p_4 - p_5) \\ p_5(p_4 - p_5) & p_5^2 & -p_4 p_5 \\ -p_4(p_4 - p_5) & -p_4 p_5 & p_4^2 \end{bmatrix} = [T_{xx}]^T \quad (13)$$

$$[T_{yy}] = \frac{t}{4a} \begin{bmatrix} (p_2 - p_3)^2 & p_3(p_2 - p_3) & -p_2(p_2 - p_3) \\ p_3(p_2 - p_3) & p_3^2 & -p_2 p_3 \\ -p_2(p_2 - p_3) & -p_2 p_3 & p_2^2 \end{bmatrix} = [T_{yy}]^T \quad (14)$$

$$[T_{yy}] = \frac{t}{4a} \begin{bmatrix} -(p_2 - p_3) & (p_4 - p_5) & p_3(p_4 - p_5) & p_2(p_4 - p_5) \\ -p_5(p_2 - p_3) & & -p_3 p_5 & p_2 p_5 \\ p_4(p_2 - p_3) & & p_4 p_3 & -p_2 p_4 \end{bmatrix} and = [T_{xy}]^T \quad (15)$$

It is noted that the sum of all the individual rows and all the individual columns of all these basic matrices are zero. This condition follows from equilibrium for all the stiffness sub-matrices, to hold for all possible material moduli. The linear combinations to obtain the stiffness sub-matrices are (Cheng and Olhoff, 1993; Pedersen, 2005):

$$[S]_{xx} = \bar{C}_{xxxx}[T_{xx}] + \bar{C}_{xyxy}\left[T_{yy}\right] + \bar{C}_{xxxy}\left(\left[T_{xy}\right] + \left[T_{xy}\right]^T\right) \quad (16)$$

$$[S]_{yy} = \bar{C}_{xyxy}\,[T_{xx}] + \bar{C}_{yyyy}\left[T_{yy}\right] + \bar{C}_{yyxy}\left(\left[T_{xy}\right] + \left[T_{xy}\right]^T\right) \quad (17)$$

$$[S]_{xy} = \bar{C}_{xxyy}\left[T_{xy}\right] + \bar{C}_{xyxy}\left[T_{xy}\right]^T + \bar{C}_{xxxy}\,[T_{xx}] + \bar{C}_{yyxy}\left[T_{yy}\right] \quad (18)$$

$$[S]_{yx} = [S]_{xy}^T \quad (19)$$

Green–Lagrange Strains in 2D Elasticity and the Involved Stiffness Matrices

Linear displacement gradients $v_{i,j}$ uses in the linear strains (Cauchy strains, Euler strains and engineering strains)$_{ij}$ by the definition of:

$$\varepsilon_{ij} := 1/2\,(v_{i.j} + v_{j.i}) \quad (20)$$

and therefore implies a constant and symmetric stiffness matrix when also the material is modeled as linearly elastic. However, the Green–Lagrange strains are non-linear and define in Cartesian tensor notation as:

$$\eta_{ij} := \frac{1}{2}\left(v_{i.j} + v_{j.i} + v_{k.i}\,v_{k.j}\right) = \varepsilon_{ij} + \frac{1}{2}\left(v_{1.i}v_{1.j} + v_{2.i}\,v_{2.j} + v_{3.i}\,v_{3.j}\right) \quad (21)$$

which mention that stiffness matrices depending on strain.

Strain and Differential Strain in Matrix Notation

The definition in matrix notation for a single component of the Green–Lagrange strain tensor is:

$$\eta_{ij} := \{B_{ij}^0\}^T\{D\} + 1/2\,\{D\}^T[B_{ij}^2]\{D\} \quad (22)$$

where $\{D\}$ gives all the nodal displacements, and the strain/displacement vector $\{B^0{}_{ij}\}$ contains the linear terms and $[B^2{}_{ij}]$ contains the non-linear terms as the symmetric strain/displacement matrix.

For finite element method $\{B^0{}_{ij}\}$ and $[B^2{}_{ij}]$ are given and will not depend on $\{D\}$. With

a differential of only $\{D\}$ Eq. (23) is therefore obtained directly from Eq. (22):

$$d\eta_{ij} = \{B_{ij}^0\}^T\{dD\} + \{D\}^T[B_{ij}^2]\{dD\} = \{B_{ij}^0\}^T\{dD\} + \{B_{ij}^L\}^T\{dD\} \quad (23)$$

i.e. the vector $\{B^L{}_{ij}\}^{\mathrm{T}} = \{D\}^{\mathrm{T}}[B^2{}_{ij}]$ depends linearly on $\{D\}$.

Collecting all strain components in strain vector notation Eqs. (22) and (23) can be written as:

$$\{\eta\} = \left([B^0] + \frac{1}{2}[B^L]\right)\{D\} = [\bar{B}]\{D\} \quad (24)$$

$$\{d\eta\} = \left([B^0] + \frac{1}{2}[B^L]\right)\{dD\} = [\bar{B}]\{dD\} \quad (25)$$

The matrix $[B^0]$ is independent of the nodal displacement $\{D\}$ while the matrix $[\mathrm{B}^{\mathrm{L}}]$ is linear dependent on $\{D\}$. $\{D\}$ gives all the nodal displacements, and the strain/displacement vector $\{B^0{}_{ij}\}$ contains the linear terms and $[B^2{}_{ij}]$ contains the non-linear terms as the symmetric strain/displacement matrix.

For Finite Element method $\{B^0{}_{ij}\}$ and $[B^2{}_{ij}]$ are given and will not depend on $\{D\}$.

Finite Element Equilibrium and Secant Stiffness Matrix

The general equilibrium that follows from the principle of virtual work is:
$\int [B]^T\{\tau\}\, dV = \{A\}$ from

$$\int \{d\eta\}^T\{\tau\}\, dV = \{\delta D\}^T\{A\} \quad (26)$$

where $\{A\}$: are given nodal loads and the resulting stresses $\{\tau\}$: are conjugated to the differential strains $\{d\eta\}$. These stresses have written in terms of resulting strains and further the resulting strains in terms of resulting displacements from Eq. (24):

$$\{\tau\} = [\bar{L}]\{\eta\} = [\bar{L}][\bar{B}]\{D\} \quad (27)$$

By the constitutive matrix $[\bar{L}]$ inserting (27) into Eq. (26) the constitutive secant relations have obtained.

$$\int [B]^T\,[\bar{L}][\bar{B}]\, dV\,\{D\} = [Ss\,]\{D\} = \{A\} \quad (28)$$

Generally the secant stiffness matrix $[\mathrm{S_s}]$ will be non-symmetric because $[B] \neq [\bar{B}]$. However, in a Newton–Raphson approach to carry out a solution to Eq. (28) we do not need invert or store this matrix. The secant stiffness matrix $[S_s]$ is the physically most important matrix because it determines the equilibrium. Note that the constitutive matrix $[\bar{L}]$ involved is the secant constitutive matrix (Pedersen, 2005).

Displacement Gradients and Results for Plane Problems

The Green–Lagrange strains for the plane problems are:

$$\eta_{xx} = \varepsilon_{xx} + \frac{1}{2}\left(v_{x.x}^2 + v_{y.x}^2\right) \quad (29)$$

$$\eta_{yy} = \varepsilon_{yy} + \frac{1}{2}\left(v_{y.y}^2 + v_{x.y}^2\right) \quad (30)$$

$$2\eta_{xy} = 2\varepsilon_{xy} + \left(v_{x.x}\, v_{x.y} + v_{y.x}\, v_{y.y}\right) \quad (31)$$

The necessary displacement gradients are $v_{x,x}, v_{y,y}, v_{x,y}$ and $v_{y,x}$, which was expressed by the displacement assumption (Eqs. (5) to (9)) in the Finite Element model are determined by:

$$v_{x.x} = \{H\}_{.x}^T[K]^{-1}\{D\}_x = \{D\}_x^T[K]^{-T}\{H\}_{.x} \quad (32)$$

$$v_{y.y} = \{H\}_{.y}^T[K]^{-1}\{D\}_y = \{D\}_y^T[K]^{-T}\{H\}_{.y} \quad (33)$$

$$v_{x.y} = \{H\}_{.y}^T[K]^{-1}\{D\}_x = \{D\}_x^T[K]^{-T}\{H\}_{.y} \quad (34)$$

$$v_{y.x} = \{H\}_{.x}^T[K]^{-1}\{D\}_y = \{D\}_y^T[K]^{-T}\{H\}_{.x} \quad (35)$$

Showing for these scalar quantities the two different forms, that are applied both for the quadratic terms needed in Eq. (30):

$$\nu^2{}_{x.x} = \{D\}^T{}_x[K]^{-T}\{H\}_{.x}\{H\}^T_{.x}[K]^{-1}\{D\}_x \quad (36)$$

$$\nu^2{}_{y.y} = \{D\}^T{}_y[K]^{-T}\{H\}_{.y}\{H\}^T_{.y}[K]^{-1}\{D\}_y \quad (37)$$

$$\nu^2{}_{x.y} = \{D\}^T{}_x[K]^{-T}\{H\}_{.y}\{H\}^T_{.y}[K]^{-1}\{D\}_x \quad (38)$$

$$\nu^2{}_{y.x} = \{D\}^T{}_y[K]^{-T}\{H\}_{.x}\{H\}^T_{.x}[K]^{-1}\{D\}_y \quad (39)$$

$$\nu_{x.x}\nu_{x.y} = \nu_{x.y}\nu_{x.x} = \{D\}^T{}_x[K]^{-T}\{H\}_{.x}1/2(\{H\}_{.x}\{H\}^T_{.y} + \{H\}_{.y}\{H\}^T_{.x})[K]^{-1}\{D\}_x \quad (40)$$

$$\nu_{y.x}\nu_{y.y} = \nu_{y.y}\nu_{y.x} = \{D\}^T{}_y[K]^{-T}\{H\}_{.y}1/2(\{H\}_{.x}\{H\}^T_{.x} + \{H\}_{.x}\{H\}^T_{.y})[K]^{-1}\{D\}_y \quad (41)$$

By the taking the symmetric part of the dyadic product $\{H\}_{,x}\{H\}^T{}_{,y}$, we obtain the equality of $v_{x,x}v_{x,y} = v_{x,y}v_{x,x}$ and of $v_{y,x}v_{y,y} = v_{y,y}v_{y,x}$. It is noticed that the products in Eq. (41) contain the same general form:

$$[t_{ij}] = [K]^{-T}\{H\}_{.i}\{H\}^T{}_{.j}[K]^{-1} \quad (42)$$

as utilized in the definition of the basic matrices of Eq. (12):

$$[Tij] = \int [tij]\, dV \quad (43)$$

From this follows that it should be possible to express the stiffness sub-matrices in terms of the basic matrices (Eqs. (13) to (15)), even with Green–Lagrange strains. However, the linear combination factors will then depend on strains and therefore need to be updated for each element (Pedersen, 2005). The stress stiffness part of the tangential stiffness matrix is expressed by the matrices $[B^2{}_{xx}]$, $[B^2{}_{yyj}]$, and $[B^2{}_{xy}]$. These matrices we get from Eqs. (29) to (41).

$$[B^2_{xx}]_x = [B^2_{xx}]_y = [t_{xx}] \quad (44)$$

$$[B^2_{yy}]_x = [B^2_{yy}]_y = [t_{yy}] \quad (45)$$

$$[B^2_{xy}]_x = [B^2_{xy}]_y = [t_{xy}] + [t_{xy}]^T \quad (46)$$

Again using the directional decomposition as illustrated by:

$$[B^2_{xx}]\{D\} = [B^2_{xx}]_x\{D\}_x + [B^2_{xx}]_y\{D\}_y \quad (47)$$

the final results obtained for the secant stiffness matrices as well as for the tangent stiffness matrices (Pedersen, 2005).

Definition of Strain from Nodal Displacement

In Figure 3, the numbering of the six nodal degrees of freedom for the element have defined. Based on these definitions short notations for displacement gradients and corresponding strains have defined.

The displacement gradients Υ_1– Υ_4 in terms of the nodal displacements d_1–d_6 are:

$$\Upsilon_1 := \nu_{x.x} = 1/2a((d_3 - d_1)p_5 - (d_5 - d_1)p_4) \quad (48)$$

$$\Upsilon_2 := \nu_{y.y} = 1/2a((d_6 - d_2)p_2 - (d_4 - d_2)p_3) \quad (49)$$

$$\Upsilon_3 := \nu_{x.y} = 1/2a\,((d_5 - d_1)p_2 - (d_3 - d_1)p_3) \quad (50)$$

$$\Upsilon_4 := \nu_{y.x} = 1/2a\,((d_4 - d_2)p_5 - (d_6 - d_2)p_4) \quad (51)$$

The linear strains such as Cauchy strains, Euler strains and engineering strains in terms of these defined displacement gradients are:

$$\varepsilon_{xx} = \Upsilon_1 \quad (52)$$

$$\varepsilon_{yy} = \Upsilon_2 \quad (53)$$

$$2\varepsilon_{xy} = \Upsilon_3 + \Upsilon_4 \quad (54)$$

and the non-linear strains (Green–Lagrange strains) are (Pedersen, 2005):

$$\eta_{xx} = \nu_{x.x} + 1/2\,(\nu^2_{x.x} + \nu^2_{y.x}) = \Upsilon_1 + 1/2\,\Upsilon_{21} + 1/2\,\Upsilon_{24} \quad (55)$$

$$\eta_{zz} = \nu_{y.y} + 1/2\,(\nu_{y.y}^2 + \nu_{x.y}^2) = \Upsilon_2 + 1/2\,\Upsilon_{22} + 1/2\,\Upsilon_{23} \quad (56)$$

$$2\eta_{xy} = (\nu_{x.y} + \nu_{y.x}) + (\nu_{x.x}\nu_{x.y} + \nu_{y.x}\nu_{y.y}) = \Upsilon_3 + \Upsilon_4 + \Upsilon_1\Upsilon_3 + \Upsilon_2\Upsilon_4 \quad (57)$$

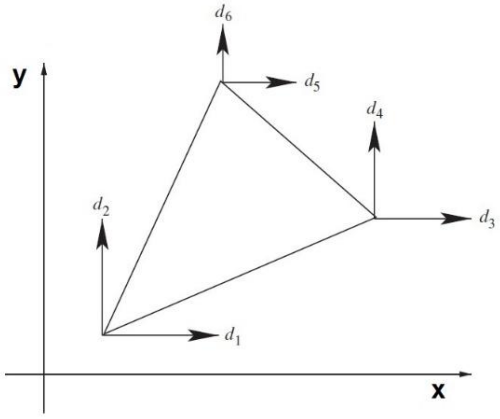

Fig. 3. Definition of nodal displacements d_1–d_6, for plane problems (Pedersen, 2005)

Analytical Sensitivity Analysis Using Adjoint Approach

In this article, the general Finite Element codes with straightforward implementation have provided with the sensitivity which, is obtained with discrete method. The adjoint method is preferred for efficiency due to the larger number of design variables compared with the system responses in nonparametric shape optimization (Wang et al., 2013). For *g* system response, *S*: is defined as a function of the design variable, *U*: is displacement vector and F: is vector of force.

So the sensitivity of *g*(*U(S),F(S),S*) with respect to *S* is defined as:

$$\frac{Dg}{Ds} = \frac{\partial g}{\partial s} + (\nabla_{ug})^T.\frac{DU}{Ds} + (\nabla_{Fg})^T.\frac{DF}{Ds} \quad (58)$$

By rewriting the governing equation as:

$$R(U(S).F(S).S) = Ks(U(S).S)\cdot U(S) - F(S) = 0 \quad (59)$$

total derivative of *R* depends in *S* is defined:

$$0 = \frac{DR}{Ds} = \frac{\partial R}{\partial s} + (\nabla_{\mathrm{u}}\mathrm{R})^T.\frac{DU}{Ds} + (\nabla_{\mathrm{F}}R)^T.\frac{DF}{Ds} = \frac{\partial Ks}{\partial s}.U + K_T.\frac{DU}{Ds} - \frac{DF}{Ds} \quad (60)$$

Introducing the adjoint variable $\lambda=[\lambda^f\ \lambda^p]^T$ by multiplying to Eq. (60) and subtraction from Eq. (58):

$$\frac{Dg}{Ds} = \frac{\partial g}{\partial s} + (\nabla_{ug})^T.\frac{DU}{Ds} + (\nabla_{Fg})^T.\frac{DF}{Ds} - \lambda^T.\left(\frac{\partial Ks}{\partial s}.U + K_T.\frac{DU}{Ds} - \frac{DF}{Ds}\right) = \frac{\partial g}{\partial s} - \lambda^T.\frac{\partial Ks}{\partial s}.U + (K_T.\lambda - \nabla_{ug})^T.\frac{DU}{Ds} + (\nabla_{Fg} + \lambda)^T.\frac{DF}{Ds} \quad (61)$$

It is always assumed that design variables are self-determining of the external force loads and prescribed displacements. So:

$$\frac{DU}{Ds} = \begin{bmatrix} DU^f/_{Ds} \\ 0 \end{bmatrix} \quad (62)$$

$$\frac{DF}{Ds} = \begin{bmatrix} 0 \\ DF^p/_{Ds} \end{bmatrix} \quad (63)$$

The third term in Eq. (61) is defined as:

$$(K_T.\lambda - \nabla_{ug})^T.\frac{DU}{Ds} = \left(\begin{bmatrix} \mathrm{K_T^{ff}} & \mathrm{K_T^{fp}} \end{bmatrix}.\begin{bmatrix} \lambda^{\mathrm{f}} \\ \lambda^{\mathrm{p}} \end{bmatrix} - \nabla_{\mathrm{U^{fg}}}\right)^T.\frac{DU^f}{Ds} \quad (64)$$

and the fourth term in Eq. (15) is define as:

$$\left(\nabla_{\mathrm{Fg}}+\lambda\right)^{T}.\frac{DF}{Ds}=(\nabla_{\mathrm{F^{pg}}}+\lambda)^{T}.\frac{DF^{p}}{Ds} \tag{65}$$

Forcing both terms in the parenthesis of Eq. (64) and Eq. (65) to zero leads to:

$$\lambda^{p}=-\nabla_{F^{pg}} \tag{66}$$

and λ^{f}: is carried out from the linear problem as:

$$K_{T}.\begin{bmatrix}\lambda^{f}\\-\nabla_{F^{pg}}\end{bmatrix}=\begin{bmatrix}K_{T}^{ff} & K_{T}^{fp}\\K_{T}^{pf} & K_{T}^{pp}\end{bmatrix}.\begin{bmatrix}\lambda^{f}\\-\nabla_{F^{pg}}\end{bmatrix}=\begin{bmatrix}\nabla_{U^{fg}}\\Y\end{bmatrix} \tag{67}$$

where *Y*: is the force vector which depend on the prescribed displacement (Wang et al., 2013).

At last, the sensitivity of response g is defined as:

$$\frac{Dg}{Ds}=\frac{\partial g}{\partial s}-\begin{bmatrix}\lambda^{f}\\-\nabla_{F^{pg}}\end{bmatrix}.\frac{\partial Ks}{\partial s}.U \tag{68}$$

Semi-Analytical Sensitivity Analysis

Sensitivity analysis has been widely applied in engineering design to explore the model response behavior, to evaluate the accuracy of a model, to test the validity of the assumptions made and etc. (Shahabian et al., 2013).

The semi-analytical method utilized to obtain the proximate partial derivatives of the secant stiffness matrix (Wang et al., 2013):

$$\frac{\partial Ks(U.s)}{\partial s}\approx\frac{\partial Ks(U.s+\Delta s)-Ks(U.s)}{\Delta s} \tag{69}$$

The approximation will be replaced by Finite Differencing based on reaction force results when the secant stiffness matrix is not present. Since the reaction force vector equals to multiply secant stiffness matrix by corresponding displacement vector, the semi-analytical could be define as:

$$\frac{\partial Ks(U.s)}{\partial s}.U\approx\frac{\partial Ks(U.s+\Delta s).U-Ks(U.s).U}{\Delta s}=\frac{F(U.s+\Delta s)-F(U.s)}{\Delta s} \tag{70}$$

Although nonlinear Finite Element analysis results the reaction force, but the approximation equilibrium avoids the direct estimate of the secant stiffness matrix. Due to the design variables used in nonparametric shape optimization usually are impressive to obtain the computational efficiency, only the semi-analytical approximation and the nonlinear analysis obtained on element level (Wang et al., 2013).

For the sensitivity analysis the following procedure is developed straightforward from Eqs. (67), (68) and (70). First to obtaining the equilibrium point *U**, the full model geometric nonlinear analysis carried out. Second, displacements $-\nabla_{F^{pg}}$ determined as boundary conditions by carrying out linear perturbation at equilibrium point *U** with external force loads. Then λ is defined as the displacement result of the analysis. For each design variable, the following steps are obtained separately. After that nodal force results from adapted neighbor elements around the design node defined in Step 1 by F(*U**,*s*), then a nonlinear analysis on the extracted small model with disturbed design node with boundary conditions *U** accomplish. This analysis results the nodal force as F(*U**,*s*+Δ*s*). Then evaluate explicit expression of *∂g/∂s*. Finally according to Eq. (68) the sensitivity of response g with the respect of design variable is obtained. The total effort for the procedure is 1 time full nonlinear analysis of the structure for a model with *M* responses and *N* design variables, (Nonlinear analysis on element

level models about each design node for *N* times plus linear perturbation analysis at the equilibrium point for M times).

Although the term $-\nabla_{F^{pg}}$ in Step 2 disappears, this procedure for sensitivities analysis of geometric nonlinear structure under external force loads is constant.

Verification and Simplifications

A number of tests are performed relative to the computational use of these analytical results. The relation between the secant and the tangential stiffness matrices are confirmed by numerical differences, treating the tangential stiffness matrix as a measure of sensitivities. In orthotropic material directions ($C_{xxxy}=C_{yyxy}=0$), and for isotropic material further simplifications $C_{yyyy}=C_{xxxx}$ and $C_{xyxy}=(C_{xxxx}-C_{xxyy})/2$) (Pedersen, 2005).

To verify the results, Results with the program were compared by another commercial finite element (ABAQUS software) that include the geometric non-linearity. Displacement of free end of the 2D cantilever beam were utilized to compare the results. These comparisons are shown in Figures (5) to (10). The results give weight to the accuracy of the modeling. It implies that the displacement obtained are approximately the same in both modeling.

CANTILEVER BEAM EXAMPLE

A 2D plain stress cantilever beam utilized as an example as shown in Figure 3a. the size of beam is 600 mm × 30 mm with the constant thickness of element "t" equals to 0.25 mm. The loads contained two prescribed displacements on the free end of cantilever beam which is not fixed, $u_{1x} = u_{2x}$ = 100 mm. specimen is meshed with a total number of 360 and 244 nodes with 2D three-node linear solid element. Mechanical properties Young's modulus and Poisson's ratio are considered 210 GPa and 0.3 respectively with the assumption of linear isotropic material. The system response is carried out as the sum of the downward reaction forces at the two points, i.e. $g = F_{1x}+F_{2x}$. x-coordinates of middle nodes of the bottom surface are considered as the design variables (red points illustrated in Figure 4b).

Numerical Results

An in-house Finite Element solver is utilized to implement the procedure. In this code, three-node linear element is used with the analytical secant and tangent stiffness matrices (Pedersen, 2006; Pedersen, 2008; DeValve and Pitchumani, 2013). The numerical results of a benchmark cantilever beam example are presented, and then the accuracy problem is discussed. (Wang et al., 2013).

Efficiency of Element Size

Figures 5 to 10 show the results of specimens with the thickness of 0.03, 0.025, 0.02, 0.015, 0.01 and 0.005 respectively. The horizontal axis shows the variations of element sizes in "Log10a" which "a" is the element size of specimens in centimeter. The vertical axis shows obtained the nonlinear displacement on the end that is not fixed in centimeter. The load on the end of cantilever beam is equal to 1000 N.

Fig. 4. a) Model description

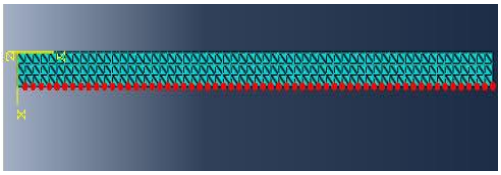

Fig. 4. b) Design nodes along the beam

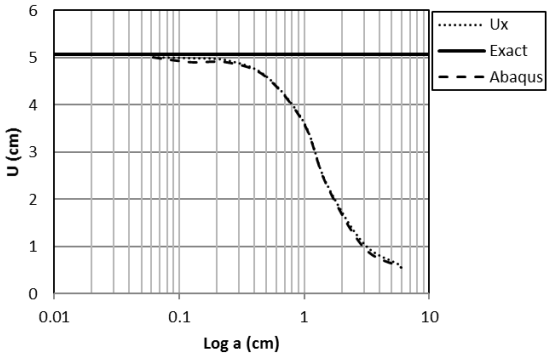

Fig. 5. Obtained non-linear displacement in *x* direction against the logarithm of the size of the element, for the specimen with the thickness of 0.03

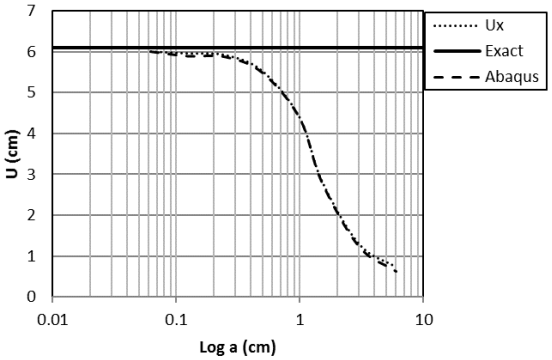

Fig. 6. Obtained non-linear displacement in *x* direction against the logarithm of the size of the element, for the specimen with the thickness of 0.025

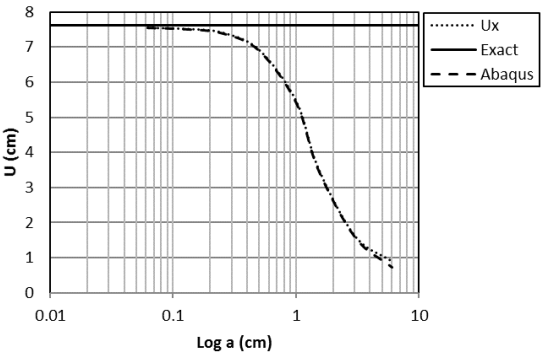

Fig. 7. Obtained non-linear displacement in *x* direction against the logarithm of the size of the element, for the specimen with the thickness of 0.02

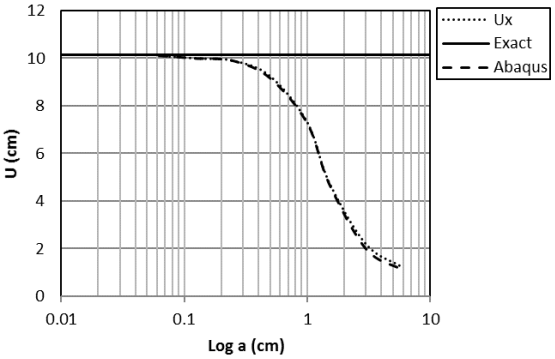

Fig. 8. Obtained non-linear displacement in *x* direction against the logarithm of the size of the element, for the specimen with the thickness of 0.015

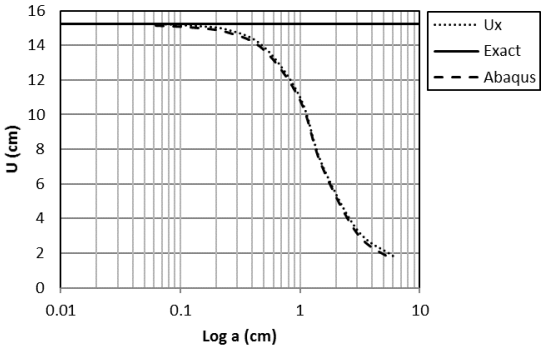

Fig. 9. Obtained non-linear displacement in *x* direction against the logarithm of the size of the element, for the specimen with the thickness of 0.01

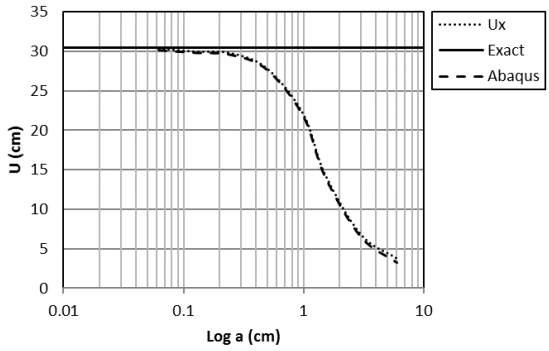

Fig. 10. Obtained non-linear displacement in *x* direction against the logarithm of the size of the element, for the specimen with the thickness of 0.005

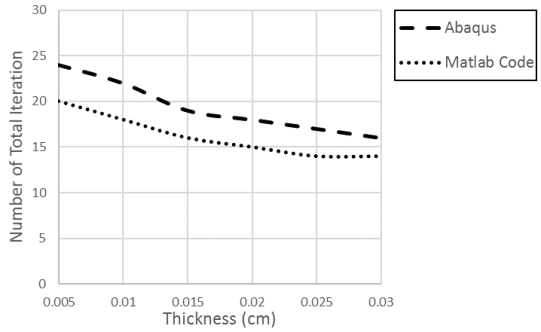

Fig. 11. Total iteration against different thicknesses for element size of 1 cm

According to the results accuracy increases by decrease of element sizes. Total iteration against different thicknesses for element size of 1 cm between MATLAB code and ABAQUS software for the specimen have been compared in Figure 11, this diagram obviously shows in this method time necessary for calculating for all thickness is decreased.

Sensitivity Results

The system response is defined as:

$$\nabla_{Ufg} = 0 \tag{71}$$

$$\nabla_{Ufg} = \begin{bmatrix} \frac{\partial g}{\partial F_{1y}} \\ \frac{\partial g}{\partial F_{2y}} \end{bmatrix} = \begin{bmatrix} 1 \\ 1 \end{bmatrix} \tag{72}$$

$$\frac{\partial g}{\partial s} = 0 \tag{73}$$

The sensitivity results are illustrated in Figure 12.

Figure 13 shows the scaled sensitivities. It is obvious that when the design nodes position is nearby the loading end (as x-coordinate increasing) the relative error increases. In linear case this phenomenon is consistent (Bletzinger, 2014; Firl and Bletzinger, 2012), which is because of the rigid "rotation" of elements.

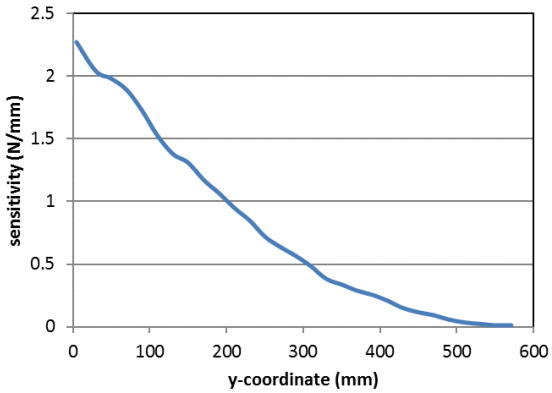

Fig. 12. Sensitivity results for specimen

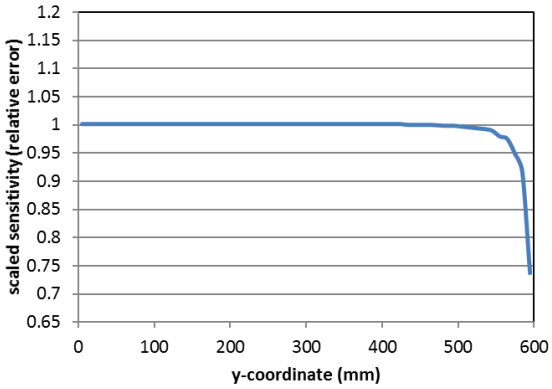

Fig. 13. Scaled sensitivity results for specimen

Efficacy of Perturbation Size and Higher Order Finite Difference Scheme

The selection of perturbation size highly influences the accuracy of sensitivity results, and to reducing the error a higher-order Finite Difference scheme will help (Wang et al., 2013; Wang et al., 2015). to apply the forward scheme method in Eq. (70) a central Finite Difference scheme is utilized:

$$\frac{\partial Ks(U^*.s)}{\partial s}.U^* \approx \frac{F(U^*.s+\Delta s) - F(U^*.s-\Delta s)}{2\Delta s} \tag{74}$$

Figure 14 compares the sensitivity result of the forward and central scheme method with different perturbation size. It is obvious that the stability of the sensitivity results well improves by the central scheme method.

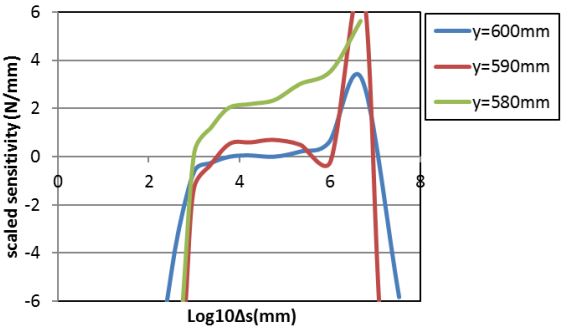

a) Analysis with forward Finite Difference scheme

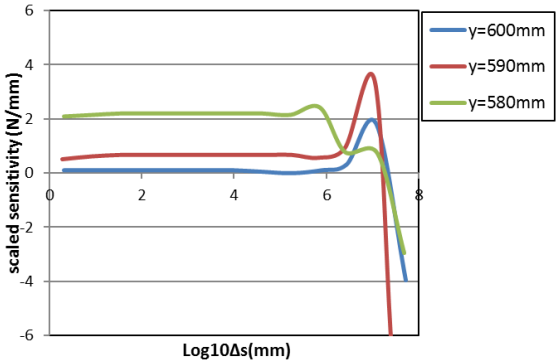

b) Analysis with central Finite Difference scheme

Fig. 14. Sensitivity results of specimen with different size of perturbation

CONCLUSIONS

In this article, the usage of formulation of secant nonlinear stiffness for discrete analytical sensitivity analysis in geometric nonlinear problem with prescribed displacements and influence of specimen mesh sizes have been investigated. A corresponding semi-analytical approach is utilized for the calculation. The procedure with MATLAB code is carried out in Finite Element and illustrated using a cantilever beam model. Higher-order Finite Difference scheme method could be greatly yield to the accuracy. To take the place of forward scheme method a central Finite Difference scheme method is performed, the stability of the sensitivity results improved by the central scheme method. Regardless of necessary time for calculating, the accuracy increase by decrease of element sizes.

REFERENCES

Bletzinger, K.U. (2014). "A consistent frame for sensitivity filtering and the vertex assigned morphing of optimal shape", *Structural and Multidisciplinary Optimization*, 49(6), 873-895.

Devalve, C. and Pitchumani, R. (2013). "A numerical analysis of carbon nanotube-based damping in rotating composite structures", *Composite Structures*, 103, 18-26.

Kim, C.J., Kang, Y.J., Lee, B.H. and Ahn, H.J. (2012). "Design sensitivity analysis of a system under intact conditions using measured response data", *Journal of Sound and Vibration*, 331(13), 3213-3226.

Cheng, G., Olhoff, N. (1993). "Rigid body motion test against error in semi-analytical sensitivity analysis", *Computers & Structures*, 46(3), 515-527.

Choi, K.K. and Kim, N.H. (2005). *Structural sensitivity analysis and optimization*, Linear System. New York: Springer Science.

De Boer, H., Van Keulen, F. (2000). "Refined semi-analytical design sensitivities", *International Journal of Solids and Structures*, 37(46), 6961-6980.

Firl, M., Bletzinger, K.U. (2012). "Shape optimization of thin walled structures governed by geometrically nonlinear mechanics", *Computer Methods in Applied Mechanics and Engineering*, 237, 107-117.

Tromme, E., Tortorelli, D., Brüls, O. and Duysinx, P. (2015). "Structural optimization of multibody system components described using level set techniques", *Structural and Multidisciplinary Optimization*, 52(5), 959-971.

Olhoff, N., Rasmussen, J. and Lund, E. (1993). "A method of ''exact'' numerical differentiation for error elimination in Fnite-Element-based semi-analytical shape sensitivity analyses", *Mechanics of Structures and Machines*, 21(1), 1-66.

Pedersen, P. (2005). "Analytical stiffness matrices with Green–Lagrange strain measure", *International Journal for Numerical Methods in Engineering*, 62(3), 334-352.

Pedersen, P., Cederkvist, J. (1981). "Analysis of non-axisymmetric vibrations and the use of basic element matrices", *Computers & Structures*, 14(3-4), 255-260.

Pedersen, P., Cheng, G. and Rasmussen, J. (1989). "On accuracy problems for semi-analytical sensitivity analysis", *Mechanics of Structures and Machines*, 17(3), 373-384.

Rezaiee-Pajand, M. and Yaghoobi, M. (2015). "Two new quadrilateral elements based on strain states",

Civil Engineering Infrastructures Journal, 48(1), 133-156.

Shahabian, F., Elachachi, S.M. and Breysse, D. (2013). "Safety analysis of the patch load resistance of plate girders: Influence of model error and variability", *Civil Engineering Infrastructures Journal*, 46(2), 145-160.

Van Keulen, F., De Boer, H. (1998). "Rigorous improvement of semi-analytical design sensitivities by exact differentiation of rigid body motions", *International Journal for Numerical Methods in Engineering*, 42(1), 71-91.

Van Keulen, F., Haftka, R.T. and Kim, N.H. (2005). "Review of options for structural design sensitivity analysis. Part 1: Linear systems", *Computer Methods in Applied Mechanics and Engineering*, 194(30), 3213-3243.

Wang, W., Clausen, P.M. and Bletzinger, K.U. (2013). "Geometric nonlinear sensitivity analysis for nonparametric shape optimization with non-zero prescribed displacements", *10th World Congress on Structural and Multidisciplinary Optimization*, May 19-4, Orlando, Florida, USA.

Wang, W. Clausen, P.M. and Bletzinger, K.U. (2015). "Improved semi- analytical sensitivity analysis using a secant stiffness matrix for geometric nonlinear shape optimization", *Computers and Structures*, 146, 143-151.

Zienkiewicz, O.C. and Taylor, R.L. (2000). *The Finite Element method*, 5th Edition, 1st, 2nd and 3rd Volumes, Butterworth-Heinemann, Oxford, U.K.